doi:10.1016/j.jmb.2008.09.045 J. Mol. Biol. (2008) 384, 540–555

JMB

Available online at www.sciencedirect.com

ScienceDirect

ELSEVIER

Zinc Binding Modulates the Entire Folding Free Energy Surface of Human Cu,Zn Superoxide Dismutase

Can Kayatekin, Jill A. Zitzewitz and C. Robert Matthews*

Department of Biochemistry and Molecular Pharmacology, University of Massachusetts Medical School, Worcester, MA 01605, USA

Received 27 May 2008; received in revised form 17 September 2008; accepted 18 September 2008
Available online
26 September 2008

Over 100 amino acid replacements in human Cu,Zn superoxide dismutase (SOD) are known to cause amyotrophic lateral sclerosis, a gain-of-function neurodegenerative disease that destroys motor neurons. Supposing that aggregates of partially folded states are primarily responsible for toxicity, we determined the role of the structurally important zinc ion in defining the folding free energy surface of dimeric SOD by comparing the thermodynamic and kinetic folding properties of the zinc-free and zinc-bound forms of the protein. The presence of zinc was found to decrease the free energies of a peptide model of the unfolded monomer, a stable variant of the folded monomeric intermediate, and the folded dimeric species. The unfolded state binds zinc weakly with a micromolar dissociation constant, and the folded monomeric intermediate and the native dimeric form both bind zinc tightly, with subnanomolar dissociation constants. Coupled with the strong driving force for the subunit association reaction, the shift in the populations toward more well-folded states in the presence of zinc decreases the steady-state populations of higher-energy states in SOD under expected *in vivo* zinc concentrations (approximately nanomolar). The significant decrease in the population of partially folded states is expected to diminish their potential for aggregation and account for the known protective effect of zinc. The ~100-fold increase in the rate of folding of SOD in the presence of micromolar concentrations of zinc demonstrates a significant role for a preorganized zinc-binding loop in the transition-state ensemble for the rate-limiting monomer folding reaction in this β-barrel protein.

Keywords: ALS; β-barrel dimer; metal binding; protein folding; thermodynamics and kinetics

Edited by P. Wright

Introduction

Amyotrophic lateral sclerosis (ALS) is a neurodegenerative disease characterized by systematic loss of the motor neurons in the brain and spinal cord.[1] Although no definitive biochemical mechanism has been discovered, a subset of familial ALS (fALS) cases has been linked to mutations at the Cu,Zn superoxide dismutase (SOD) locus.[2,3] Despite constituting only 2%–5% of all known cases, SOD-mediated fALS is the most prominent identified heritable cause of the disease. Moreover, sporadic cases of ALS are clinically and pathologically similar to fALS cases,[1] suggesting that both forms may share a common underlying mechanism.

In its native form, SOD is a 153-aa cytosolic protein that catalyzes the dismutation of superoxide into hydrogen peroxide and oxygen.[4] SOD is catalytically active as a homodimer with both a copper ion and a zinc ion bound to each monomer. The fold of an SOD monomer is a β-sandwich composed of eight antiparallel β-strands supporting a pair of large loops that follow β4 and β7—loops IV and VII, respectively (Fig. 1). Loop IV is covalently linked to β8 by a disulfide bond between Cys57 and Cys146.[6]

*Corresponding author. E-mail address: C.Robert.Matthews@umassmed.edu.

Abbreviations used: AEDANS, 5-[[2-(acetylamino) ethyl]amino] napthalene-1-sulfonic acid; ALS, amyotrophic lateral sclerosis; AS-SOD, C6A/C111S SOD; fALS, familial amyotrophic lateral sclerosis; FRET, Förster resonance energy transfer; Gdn-HCl, guanidine hydrochloride; mAS-SOD, F50E/G51E/C6A/C11S monomeric variant of SOD; SOD, human Cu,Zn superoxide dismutase; TCEP, Tris(2-carboxyethyl) phosphine; TSE, transition-state ensemble.

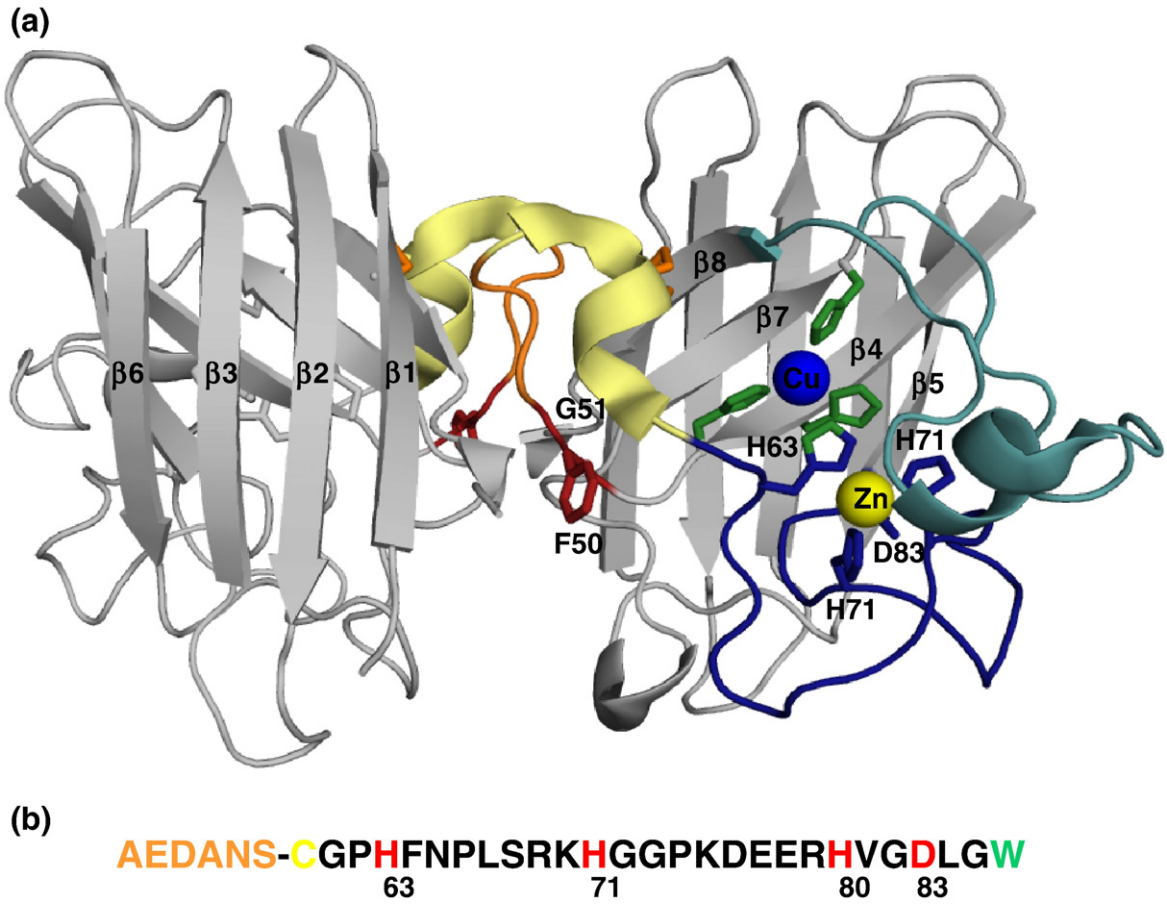

Fig. 1. (a) The crystal structure of SOD (Protein Data Bank code 2C9V).[5] The zinc ion is depicted in yellow, with the metal-binding region of the zinc-binding loop (loop IV), as well as the residues that bind zinc, shown in dark blue. Proximal to this region, the electrostatic loop is shown in teal. The region of loop IV involved in or near the intramolecular disulfide bond (in dark orange) between C57 and C146 is shown in light yellow, and the dimer interface portion of loop IV is highlighted in orange. Shown in blue is the copper ion, with the histidines to which it binds depicted in green. In red are F50 and G51, which were replaced with glutamic acid to create mAS-SOD. (b) The sequence of the zinc-binding loop with the zinc-binding residues indicated in red. The nonnative residues are shown in teal for the C-terminal tryptophan and in yellow for the N-terminal cysteine, which was further modified with an AEDANS molecule.

Loops IV and VII coordinate the metals and provide the catalytic and electrostatic components of the active site.[7] The copper redox cycle drives the disproportionation reaction, and the zinc ion is thought to play a role in defining the structure and stability of SOD.[8–10] The binding of zinc to dimeric SOD is very tight, with a $K_d < 10^{-8}$ M by isothermal titration calorimetry[11] and a K_d of $\sim 10^{-14}$ M by competition experiments.[12] While the order of the metal-binding and disulfide-bonding events *in vivo* is not definitively known, it is thought that zinc binds to the disulfide-reduced protein first. This complex then interacts with the copper chaperone of SOD, which loads the copper and oxidizes the intramolecular disulfide bond.[13]

Although several hypotheses have been proposed to explain the toxic gain of function of SOD variants,[14–17] a prevailing view holds that amino acid replacements increase populations of partially folded states and induce subsequent aggregation.[14,18,19] The rationale for the unfolding/aggregation hypothesis is based on the fact that well over 100 replacements and C-terminal truncations†, covering nearly 50% of the sequence, can cause ALS.[20] Many of these variants lead to the deposition of amorphous aggregates in and around the motor neurons of patients afflicted with ALS, and a debate has ensued about whether small oligomers or macroscopic aggregates are the toxic agents.[21] It has been demonstrated that loss of zinc may result in aggregation, reinforcing the structural importance of zinc.[22] Candidates for aggregation have focused on zinc-free partially folded monomeric states of SOD, including those with the disulfide bond intact and those in which the disulfide bond has been reduced.[23] More recently, the unfolded state, extruded from the ribosome and prior to disulfide-bond formation or folding, has also been proposed as a candidate for aggregation and toxicity.[24]

† See http://alsod.iop.kcl.ac.uk/Als/ for a complete list.

The unfolding/aggregation hypothesis has been tested by comparative biophysical analysis of the thermodynamic folding properties of wild-type and ALS-inducing SOD variants in both their disulfide-oxidized[25] and disulfide-reduced[26,27] forms. Detailed analyses of the folding mechanisms of disulfide-intact SOD have shown that both apo-SOD[26,28,29] and holo-SOD[30] fold by a three-state mechanism involving a folded monomeric intermediate. Left unanswered in these studies were several questions on the specific role of zinc on the folding and stability of SOD that pertain to its influence on nonnative states that might be responsible for aggregation. Pertinent to the argument that newly synthesized chains might be the source of toxicity, at what stage of folding does zinc become bound to SOD? Once the native state is reached, what are the quantitative ramifications of zinc binding to diminish the propensity of the disulfide-bonded native dimer and the folded monomer to populate less-structured, aggregation-prone states? In the event that the folded monomer is a source of aggregation, does zinc binding alter the relative populations of monomeric and dimeric forms of SOD at equilibrium to favor the fully folded form? A comparative analysis of the thermodynamic and kinetic folding properties of disulfide-bonded C6A/C111S SOD (AS-SOD) in the presence and in the absence of zinc demonstrated that zinc binding modulates its entire folding free energy surface. The results provide a benchmark for future studies on metal-binding ALS-inducing variants containing disulfide bonds and on disulfide-reduced SOD.

Results

Quantitative information on the effect of zinc binding on high-energy states in SOD was obtained by chemical denaturation analysis of both the thermodynamic and kinetic properties of the reversible folding reaction. The C6A/C111S variant, AS-SOD, was used in place of the wild-type SOD because it has been shown to fold reversibly with wild type-like stability.[31] The elimination of the free cysteines precludes intermolecular disulfide-bond formation and intramolecular disulfide-bond interchange. The results obtained can be compared with those from a previous study of metal-free apo-AS-SOD[28] to determine the decrease in the free energy (i.e., the increase in stabilization relative to the unfolded state) of the zinc-bound states in the absence of denaturant.

Thermodynamic analysis

Chemical denaturation of dimeric AS-SOD

The effects of zinc binding on the thermodynamic properties of disulfide-intact AS-SOD were determined by chemical denaturation experiments in the presence and in the absence of zinc and monitored by circular dichroism (CD) spectroscopy. It has been previously shown that the ellipticity at 230 nm is a sensitive probe of global structure in AS-SOD[28] and provides optimal signal to noise compared with measurements at the typical minimum for β-rich structures of 218 nm. Although urea is a sufficiently potent denaturant to unfold apo-SOD,[28,32] guanidine hydrochloride (Gdn-HCl) was required to unfold zinc-bound AS-SOD. The Gdn-HCl unfolding titration curves at 230 nm, pH 7.2, and 20 °C for apo- and stoichiometric zinc-bound Zn-AS-SOD (two zinc ions per dimer) are shown in Fig. 2. The native dimeric form of apo-AS-SOD is stable up to ~1 M Gdn-HCl, where it experiences a cooperative unfolding transition that is complete by ~2 M Gdn-HCl. In the presence of stoichiometric zinc, Zn-AS-SOD is stable up to ~2 M Gdn-HCl, where it also undergoes a cooperative unfolding transition that is complete by ~3 M Gdn-HCl. The reversibility of the Zn-AS-SOD unfolding reaction was demonstrated by the coincidence of a refolding transition curve beginning with denatured AS-SOD (data not shown). As has been observed previously with holo-SOD,[30] full equilibration of the Zn-AS-SOD samples at pH 7.2 for both unfolding and refolding curves was exceedingly slow, requiring 7 days at room temperature.

Chemical denaturation of monomeric AS-SOD

Previous analyses of the chemical denaturation of apo-SOD[28] and holo-SOD[30] have implicated an essential role for a folded monomeric species that subsequently undergoes a diffusion-limited association reaction to produce the native dimer. Insight into the effect of zinc binding on the stability of the monomeric folding intermediate was obtained by examining the enhancement of stability for a stable monomeric version of AS-SOD, mAS-SOD, upon zinc binding. The mAS-SOD variant was created by replacing two subunit interface residues, F50 and

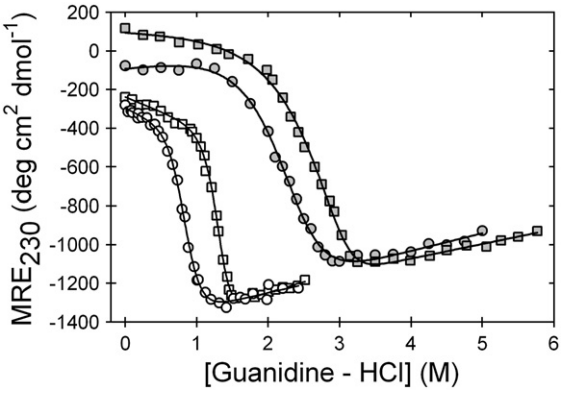

Fig. 2. Equilibrium Gdn-HCl titrations measured by ellipticity in 20 mM Hepes, pH 7.2, at 20 °C. Representative data at 230 nm are shown with fits to a two-state model for the metal-free apo-AS-SOD (open squares) and apo-mAS-SOD (open circles) and with fits to a three-state model for stoichiometric Zn-AS-SOD (filled squares) and Zn-mAS-SOD (filled circles). Protein and zinc concentrations were 10 μM for AS-SOD and 5 μM for mAS-SOD.

G51, with glutamic acid.[33] In the absence of zinc, the native mAS-SOD is stable up to ~0.7 M Gdn-HCl, where it undergoes a cooperative unfolding transition that is complete by ~1 M Gdn-HCl. Similar to AS-SOD, the addition of stoichiometric zinc to mAS-SOD (one zinc per chain) significantly stabilizes the protein. Zn-mAS-SOD is stable up to ~1.5 M Gdn-HCl, where it undergoes a cooperative unfolding transition that is complete by ~2.8 M Gdn-HCl.

Stoichiometry and location of zinc binding to AS-SOD

Inspection of the titration curves in Fig. 2 reveals a distinctly more positive ellipticity at 230 nm under native conditions for the stoichiometric Zn-AS-SOD and possibly for Zn-mAS-SOD compared with their metal-free counterparts. Realizing that this signal could be used to monitor zinc binding to the folded dimeric form of AS-SOD, the ellipticity at 230 nm was monitored as a function of zinc concentration. The ellipticity increased linearly with increasing concentrations of zinc up to the level at which the stoichiometric zinc concentration was reached (Fig. 3). Further addition of zinc led to a decrease in the ellipticity that is complete when an equivalent of six zinc ions per dimer has been added. The data imply that zinc binds to at least two sites on apo-AS-SOD, possibly the zinc and copper sites nested in loops IV and VII (Fig. 1).

The assumption that the initial increase in ellipticity upon addition of zinc corresponds to zinc binding at the zinc site was tested using cobalt ion as an optical probe. Cobalt is an excellent mimic for zinc because its divalent form has an ionic radius and geometric preferences that are similar to those for zinc. Although zinc is spectroscopically silent, cobalt gives strong absorbance in the visible region when bound to the zinc site in SOD. Addition of stoichiometric cobalt to apo-AS-SOD yielded strong absorption bands between 500 and 650 nm, very similar to the previously determined spectra of cobalt ion bound to the zinc site (Fig. 4).[34] By contrast, the addition of stoichiometric cobalt after apo-AS-SOD was preincubated with stoichiometric zinc resulted in dramatically reduced absorption bands (Fig. 4); further addition of zinc eliminated the small residual absorption band. These data show that zinc binds preferentially to the zinc site on AS-SOD. Excess zinc binds to one or more additional sites, possibly the copper site, on each subunit. Crystallographic studies of SOD in the presence of excess zinc show zinc can bind to the copper site[5] and cobalt binding to the copper site produces an absorption band in this same region.[34] This conclusion is also consistent with the findings of an extensive dialysis against buffer of a sample of AS-SOD preincubated with 10-fold excess zinc. Atomic absorption analysis revealed an average of 2.5 zinc ions per dimer, implying a second weaker binding site for zinc in AS-SOD.

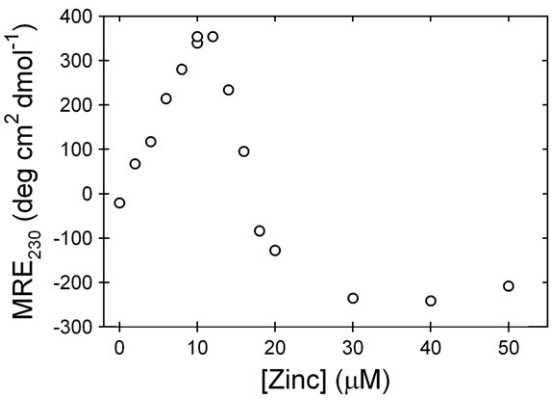

Fig. 3. Titration of AS-SOD in buffer monitoring the change in ellipticity at 230 nm as a function of the zinc concentration. The titration was performed in 20 mM Hepes, pH 7.2, at 20 °C. Protein concentration was 10 μM.

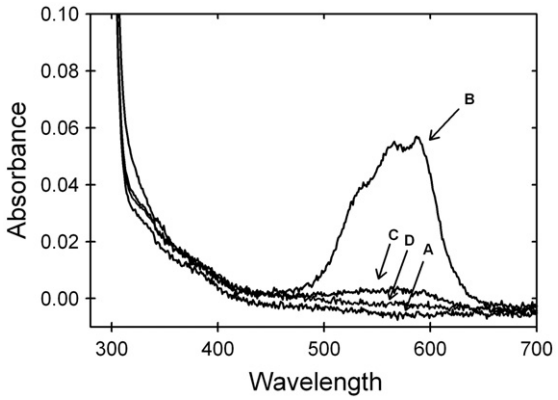

Fig. 4. Visible absorbance spectra of AS-SOD in 20 mM Hepes, pH 7.2, at room temperature. Traces shown are protein (A) with no metal added, (B) after addition of one cobalt ion per monomer, (C) after preincubation of protein with one zinc ion per monomer followed by the addition of one cobalt ion per monomer, and (D) after preincubation with six zinc ions per monomer followed by the addition of one cobalt ion per monomer. The protein concentration for all four traces was 123 μM.

Zinc binding to unfolded AS-SOD

Although it is not surprising that the folded state of AS-SOD binds zinc in the zinc site with high affinity, it is possible that the unfolded state may also bind zinc. Previous studies on azurin[35,36] found that zinc can bind to the chemically denatured protein, complicating estimates of stability by denaturation experiments. Binding to the unfolded state of AS-SOD was tested by synthesizing a 27-residue peptide that corresponds to the sequence containing all four zinc-binding side chains—H63, H71, H80, and D83 (Fig. 1b). The potential acquisition of structure upon zinc binding to the peptide was monitored by Förster resonance energy transfer (FRET) from a tryptophan added at the C-terminus to a 5-[[2-(acetylamino)ethyl]amino] napthalene-1-sulfonic acid (AEDANS) acceptor covalently attached to an additional cysteine at the N-terminus.

As shown in Fig. 5a, the fluorescence intensity of tryptophan emission at 360 nm decreased and that of AEDANS emission at 500 nm increased with increasing zinc concentrations. The quenching of the tryptophan donor by the AEDANS acceptor implies that zinc induces structure in the peptide in the micromolar concentration range. The affinity of this peptide for zinc was calculated by fitting the data in buffer to a simple binding isotherm (Fig. 5b). The dissociation constant of the zinc–peptide complex is 1.1±0.1 μM, and the free energy of binding is −8.0± 0.3 kcal (mol monomer)$^{-1}$ at the standard state (1 M in each component). Relevant to the denaturation analysis of AS-SOD, the binding becomes progressively weaker in the presence of increasing Gdn-HCl concentrations to over 60 μM at 4 M Gdn-HCl. Significant zinc binding to the peptide is not detected above 5 M Gdn-HCl (Fig. 5b). A plot of $-RT \ln(K_d)$ (i.e., the free energy of the dissociation reaction at the standard state ΔG^0_d) *versus* the concentration of Gdn-HCl is linear (Fig. S1). This behavior is typical of protein folding reactions when the free energy of folding is plotted *versus* the concentration of denaturant. The free energy of the dissociation reaction in the absence of denaturant, ΔG^0_d, obtained by extrapolation, −7.6 kcal (mol monomer)$^{-1}$, agrees well with the value obtained by direct measurement, −8.0 kcal (mol monomer)$^{-1}$, and the denaturant dependence of ΔG^0_d, the *m* value, is 0.42 kcal (mol monomer)$^{-1}$ M^{-1} (Table 1). Thus, under equilibrium conditions, there is a significant perturbation of the free energy of the unfolded state of SOD from zinc binding to the zinc-binding loop peptide. This behavior influences the Gdn-HCl unfolding reaction of SOD and must be accounted for in the extraction of accurate thermodynamic parameters (see below).

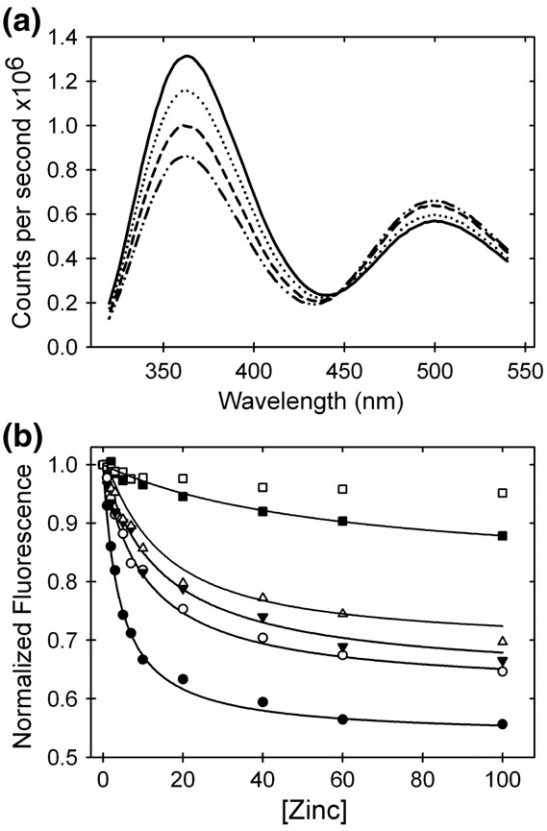

Fig. 5. Zinc-binding affinity of a peptide model of the unfolded state of SOD. The change in fluorescence intensity of a FRET pair at the termini of a peptide encompassing the four zinc-binding residues of SOD was monitored at various zinc concentrations and in the presence of varying amounts of Gdn-HCl. (a) The addition of zinc causes a decrease in the tryptophan fluorescence (λ_{max}=360 nm) and a proportional increase in AEDANS fluorescence (λ_{max}=500 nm). Traces shown are at 1 M Gdn-HCl and represent zinc concentrations of 1 μM (continuous line), 7 μM (dotted line), 20 μM (dashed line), and 60 μM (dashed and dotted line). (b) Quenching of the tryptophan emission at 360 nm by AEDANS as zinc induces structure in the peptide of the zinc-binding loop. The isotherms shown are for 0 M Gdn-HCl (filled circles), 0.5 M Gdn-HCl (open circles), 1 M Gdn-HCl (filled inverted triangles), 2 M Gdn-HCl (open triangles), 4 M Gdn-HCl (filled squares), and 5 M Gdn-HCl (open squares). These data represent two preparations of the peptide with different labeling efficiencies such that the intensities were normalized to the zinc-free value to show relative differences. The peptide concentration for all experiments was 4 μM in 20 mM Hepes, pH 7.2, and 20 °C.

Thermodynamic parameters for AS-SOD and Zn-AS-SOD

The evident cooperativity of the Gdn-HCl unfolding reaction and the results of previous studies on apo-AS-SOD denatured in urea[28] motivated the test of a simple two-state equilibrium model for the unfolding of apo-AS-SOD, $2U \leftrightarrows N_2$, and a three-state equilibrium model for Zn-AS-SOD with Gdn-HCl, $2U + 2Zn \leftrightarrows 2(U{\cdot}Zn) \leftrightarrows (N{\cdot}Zn)_2$. The latter fits were done by fixing the change in free energy in the absence of denaturant and the *m* value for the $2(U{\cdot}Zn) \leftrightarrows 2U + 2Zn$ step to twice the values obtained from the Zn–peptide complex described above. The accuracy of the parameters was enhanced by simultaneously fitting all the CD data between 220 and 240 nm to the models for both forms (see Materials and Methods for a more detailed description of the analysis).

The stability of the apo-AS-SOD at standard-state concentrations (1 M in each of the components), at 20 °C and pH 7.2, is −18.6±0.3 kcal (mol dimer)$^{-1}$ (Fig. 2; Table 1), in good agreement with the previously determined value by Gdn-HCl denaturation monitored by CD, −17±2 kcal (mol dimer)$^{-1}$,[29] as well as with the value determined by urea denaturation monitored by CD, −20.4±1.0 kcal (mol dimer)$^{-1}$.[28] The denaturant dependence of the free energy difference between the folded dimer and the unfolded monomer, the *m* value, is 9.3±0.2 kcal (mol dimer)$^{-1}$ M^{-1}.

The binding of zinc increases the stability of AS-SOD, as evidenced by the increase in the apparent midpoint of the unfolding transition from ~1.3 to ~2.6 M Gdn-HCl (Fig. 2). Fitting the titration data to the three-state model, $2U + 2Zn \leftrightarrows 2(U{\cdot}Zn) \leftrightarrows (N{\cdot}Zn)_2$,

Table 1. Thermodynamic parameters measured at 20 °C and pH 7.2 for the Gdn-HCl-induced equilibrium unfolding reactions of dimeric and monomeric apo- and zinc-bound AS-SOD and the zinc titration of the peptide of the zinc-binding region of SOD

	Kinetic ΔG^0	Equilibrium ΔG^0	*m* value Kinetic	*m* value Equilibrium	K_d
Apo-mAS-SOD[a]	−3.6±0.1	−4.3±0.1	4.9±0.3	5.1±0.5	NA[b]
Apo-AS-SOD[c]	−20.9±0.3	−18.6±0.3	ND[d]	9.3±0.2	NA
Zn-mAS-SOD[a]	−17.0±0.7	−13.4±0.6	4.6±0.3	2.6±0.2	100±122 pM[e]
Zn-AS-SOD[c]	−49.4±1.5	−33.0±1.4	ND	4.2±0.3	22±35 pM[e]
Peptide[a]	NA	−8.0±0.3	NA	0.42±0.08	1.1±0.1 μM

[a] Units for ΔG^0 are shown in kcal (mol monomer)$^{-1}$; those for *m*, kcal (mol monomer)$^{-1}$ M^{-1}.
[b] Not applicable.
[c] Units for ΔG^0 are shown in kcal (mol dimer)$^{-1}$; those for *m*, kcal (mol dimer)$^{-1}$ M^{-1}.
[d] The *m* value could not be calculated because the protein concentration-dependent kinetic data in the transition region were inaccessible in Gdn-HCl.
[e] Calculated from kinetic parameters.

the free energy change and the *m* value for the 2 (U▪Zn) ⇆ $(N▪Zn)_2$ reaction were found to be −17.0±0.2 kcal (mol dimer)$^{-1}$ and 3.4±0.1 kcal (mol dimer)$^{-1}$ M^{-1}, respectively. When the free energy change for this reaction is added to that for the 2U + 2Zn ⇆ 2(U▪Zn) reaction, −16.0±1.2 kcal (mol dimer)$^{-1}$, the total free energy difference between the $(N▪Zn)_2$ and 2U + 2Zn states is −33.0±1.4 kcal (mol dimer)$^{-1}$ at the standard state.

Surprisingly, the sum of the *m* values for the folding/subunit dissociation step, 3.4±0.1 kcal (mol dimer)$^{-1}$ M^{-1}, and twice the *m* value for the zinc dissociation step, 0.84 kcal (mol dimer)$^{-1}$ M^{-1}, of 4.2±0.3 kcal (mol dimer)$^{-1}$ M^{-1} is significantly lower than the *m* value for apo-SOD of 9.3±0.2 kcal (mol dimer)$^{-1}$. The magnitude of the *m* value has been shown to correlate with the exposure of buried surface area during unfolding.[37] Therefore, if zinc binding induces structure in native SOD, one might expect that the total *m* value for the dimer unfolding and zinc dissociation steps would be at least equal to if not in excess of the *m* value for the unfolding of apo-SOD. As shown below, the aberrant *m* value for the unfolding of AS-SOD in the presence of stoichiometric zinc has another explanation.

Thermodynamic parameters for mAS-SOD and Zn-mAS-SOD

The stability enhancement for zinc binding to mAS-SOD was obtained by similar two-state and three-state fits of the unfolding titration data (Fig. 2) for the apo- and zinc-bound stable monomeric forms (see Materials and Methods). The stability of apo-mAS-SOD, −4.3±0.1 kcal (mol monomer)$^{-1}$ (Table 1), is in good agreement with the value previously determined by urea denaturation, −4.27±0.48 kcal (mol monomer)$^{-1}$. The *m* value for the monomer unfolding reaction is 5.1±0.5 kcal (mol monomer)$^{-1}$ M^{-1}. The free energy change for the (U▪Zn) ⇆ (M▪Zn) reaction is −5.8±0.3 kcal (mol monomer)$^{-1}$, and the *m* value is 2.3±0.1 kcal (mol monomer)$^{-1}$. When zinc binding to the unfolded state is considered, the total free energy change for the (M▪Zn) ⇆ U + Zn reaction is −13.4±0.6 kcal (mol monomer)$^{-1}$, and the total *m* value is 2.6±0.2 kcal (mol monomer)$^{-1}$ M^{-1}. Similar to Zn-AS-SOD, the *m* value for the unfolding of the zinc-bound stable monomeric form is significantly less than its apo-mAS-SOD counterpart.

There are several possibilities for the discrepancies in the *m* values for the apo- and zinc-bound forms of AS-SOD and mAS-SOD. The reduced *m* values in the presence of zinc could reflect the population of additional species in the transition region. Obvious candidates are the metal-free N state and zinc bound to non-zinc sites—possibly the copper site—evident at superstoichiometric zinc concentrations (Fig. 3). The possibility that zinc-bound monomers are populated is unlikely since both AS-SOD and mAS-SOD exhibit the same behavior. Kinetic analysis of the AS-SOD folding reaction resolves the discrepancies between the *m* values and provides reliable estimates of the thermodynamic parameters sought in this study.

Kinetic analysis

Thermodynamic analysis of the equilibrium unfolding reactions of AS-SOD, mAS-SOD, and a peptide model for the zinc-binding loop has shown that zinc can bind to all three species in the kinetic folding mechanism. Kinetic folding studies are required to determine the effects of zinc binding on the intervening transition states. Importantly, kinetic analysis also provides an alternative approach toward determining the magnitude of the stabilizing effect of zinc on the monomeric and dimeric forms of AS-SOD.

Folding kinetics of AS-SOD and Zn-AS-SOD

Semi-log plots of the relaxation times as a function of the final denaturant concentration, chevron plots,[38] for apo-AS-SOD and Zn-AS-SOD are shown in Fig. 6a. The single unfolding relaxation time for dimeric apo-AS-SOD decreases exponentially above 3 M Gdn-HCl, and the single refolding relaxation time decreases exponentially below 1 M Gdn-HCl. Neither phase depends on the protein

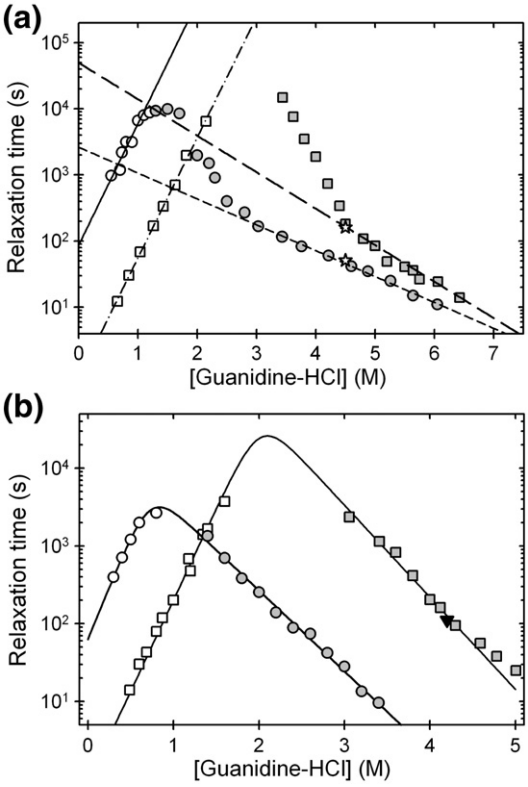

Fig. 6. Observed refolding (open symbols) and unfolding (filled symbols) relaxation times for (a) AS-SOD and (b) mAS-SOD as a function of final Gdn-HCl concentration in the presence (squares) and in the absence (circles) of zinc as monitored by CD at 230 nm. In (a), the solid and dashed and dotted lines represent the linear extrapolations used to determine the relaxation times for the rate-limiting folding reactions, and the dashed lines represent the extrapolations used to determine the dimer dissociation reaction in the absence of denaturant. In (b), the lines represent the fits of the data to simple two-state chevrons. The results yield the unfolding and refolding relaxation times and their reciprocal rate constants in the absence of denaturant. The two observed relaxation times of the unfolding of one zinc per dimer AS-SOD are shown by the open star symbols in (a). The filled inverted triangle in (b) is the observed relaxation time for the unfolding double-jump experiment at stoichiometric zinc concentration. Protein concentration was 10 μM for both AS-SOD and mAS-SOD, and the buffer contained 20 mM Hepes, pH 7.2, 20 °C.

concentration under strongly unfolding or refolding conditions (data not shown). Previous studies of the urea denaturation reaction for apo-AS-SOD[28] have shown that the unfolding phase at high denaturant concentration corresponds to the unimolecular dissociation of the dimer. The single refolding phase observed by CD at 230 nm corresponds to the rate-limiting folding of the monomer. The nonexponential dependence in the unfolding leg of the chevron between 1.5 and 3 M Gdn-HCl reflects the coupling of the monomer refolding/unfolding and the dimer association/dissociation reactions in the transition zone.[28]

The presence of zinc has a significant effect on both the unfolding and refolding reactions of AS-SOD (Fig. 6a; Table 2). Unfolding is slowed by 5-fold at 6 M Gdn-HCl, and refolding is accelerated by a factor of ~100-fold at 0.6 M Gdn-HCl. The denaturant dependence of the dimer dissociation relaxation time in the presence of zinc between 5.5 and 6.8 M Gdn-HCl, -0.95 ± 0.06 kcal (mol dimer)$^{-1}$ M^{-1}, is larger than that for apo-AS-SOD between 3.8 and 6.0 M Gdn-HCl, -0.67 ± 0.03 kcal (mol dimer)$^{-1}$ M^{-1}. As a result, the dimer dissociation relaxation time in the absence of denaturant, as estimated by linear extrapolation, is 20-fold longer in the presence of zinc. The small increase in the denaturant dependence of the relaxation time implies an enhancement of structure as the zinc-binding and electrostatic loops are organized by zinc binding. Given the quite similar denaturant dependence of the refolding relaxation times for apo- and Zn-AS-SOD, the kinetic refolding data yield a 100-fold acceleration of the refolding rate by zinc in the absence of Gdn-HCl. Although the linear extrapolations in Gdn-HCl may be questioned,[39] the differences between the extrapolated relaxation times in the presence and in the absence of zinc should be minimal.

Potter *et al.*,[11] on the basis of isothermal titration calorimetry experiments, have proposed that the binding of the first zinc ion to the SOD dimer may contribute the majority of the stability induced by zinc binding. By implication, the one-zinc-per-dimer species should comprise the entire population at half-saturation. This conclusion was investigated by incubating AS-SOD with one zinc ion per dimer and monitoring the unfolding reaction. The observed unfolding reaction could not be fit to a single exponential expected for a homogeneous population. When fit to two exponentials, the observed relaxation times corresponded well with the unfolding relaxation times of the apo- and zinc-bound proteins (Fig. 6). This result is better explained by a binomial distribution of zinc in the two zinc sites per dimer, reflecting the metal-free protein, the half-saturated protein, and the fully saturated protein. The absence of a third phase suggests that the unfolding relaxation time of the one-zinc-per-dimer species is similar to that of the two-zinc ions-per-dimer species. As noted above, the unfolding of AS-SOD incubated with two zinc ions per dimer is well described by a single exponential at the same concentration of Gdn-HCl (Fig. 6). The discrepancies between these results and those from the laboratory of Potter *et al.* may reflect the different pH values at which the two studies were performed. It is likely that the histidines that ligate zinc are protonated at pH 5.5, at which the isothermal titration calorimetry studies were done. The zinc-binding properties would undoubtedly be altered from those at pH 7.2, perhaps to include a preferential binding of the first zinc ion to the dimeric protein.

Attempts to visualize the protein concentration dependence in the transition region, 1.5–3.0 M Gdn-HCl, as previously observed for the urea denaturation reaction[26,28] and required for the determination

Table 2. Microscopic rate constants, kinetic $m^{\ddagger}$ values, and the effect of zinc binding on the activation free energy of the TSEs of AS-SOD measured at 20 °C and pH 7.2

	Apo-AS-SOD[a]	Zn-AS-SOD[a]	$\Delta G^{\ddagger}$ Apo-AS-SOD[b]	$\Delta G^{\ddagger}$ Zn-AS-SOD[b]	$\Delta\Delta G^{\ddagger}$[b]
k_f[c]	0.012±0.002	1.19±0.05	5.2±0.2	0.2±0.08	−5.0±0.1
$m_f^{\ddagger}$[c]	3.17±0.53	3.13±0.01	NA[d]	NA	NA
k_u[e]	$(3.1\pm1.5)\times10^{-5}$	$(2.0\pm1)\times10^{-7}$	−12.0±0.6	−18.0±0.6	6.0±0.7
$m_u^{\ddagger}$[e]	−1.39±0.07	−1.45±0.11	NA	NA	NA
k_a[f]	$(6.9\pm8.3)\times10^{6}$	$(6.9\pm8.3)\times10^{6}$	18.2±1.2	18.2±1.2	0
$m_a^{\ddagger}$	ND[g]	ND	NA	NA	NA
k_d[h]	$(38.1\pm0.9)\times10^{-5}$	$(2.1\pm0.4)\times10^{-5}$	−4.6±0.1	−6.3±0.1	1.7±0.1
$m_d^{\ddagger}$[h]	−0.67±0.03	−0.95±0.06	NA	NA	NA

[a] Units for the monomer folding rate constants (k_f), unfolding rate constants (k_u), dimer association rate constants (k_a), and dimer dissociation rate constants (k_d) are shown in s^{-1}; those for the denaturant dependence of monomer folding ($m_f^{\ddagger}$) and unfolding ($m_u^{\ddagger}$) rate constants, in kcal (mol monomer)$^{-1}$ M^{-1}; and those for the denaturant dependence of the dimer dissociation rate constant ($m_d^{\ddagger}$), in kcal (mol dimer)$^{-1}$ M^{-1}.
[b] Units for the activation free energy barrier ($\Delta G^{\ddagger}$) and the change in the free energy barrier upon zinc binding to the TSE ($\Delta\Delta G^{\ddagger}$) are shown in kcal (mol dimer)$^{-1}$.
[c] Calculated from the linear extrapolation of the refolding leg of the AS-SOD chevron (Fig. 6a).
[d] Not applicable.
[e] Calculated from the two-state fit of the mAS-SOD chevron (Fig. 6b).
[f] The dimer association rate constant was taken from A.-K. E. Svensson *et al.* (manuscript in preparation).
[g] Not determined.
[h] Calculated from the linear extrapolation of the >5.5 M Gdn-HCl region of the unfolding leg of the zinc-bound AS-SOD chevron and the >3.8 M Gdn-HCl region of the unfolding leg of the apo-AS-SOD chevron (Fig. 6a).

of the association rate constant, were not successful. The relaxation times in this Gdn-HCl concentration range exceed experimental limitations, $>10^5$ s, precluding accurate measurements.

Folding kinetics for mAS-SOD

In the absence of direct information on the association reaction, the effect of zinc binding on refolding/unfolding reactions of the stable monomer, mAS-SOD, was examined. Lindberg *et al.*[25] used this approach toward partitioning the global free energy change for the unfolding of AA-SOD into its monomer folding reaction and monomer/dimer association reaction components. In the absence of zinc, apo-mAS-SOD unfolds via a simple exponential reaction whose relaxation time decreases linearly with increasing denaturant concentrations, from ~1 to ~3.5 M Gdn-HCl (Fig. 4B). The single refolding relaxation time decreases linearly with decreasing Gdn-HCl below ~1 M denaturant, and the two legs of the chevron intersect at ~1 M Gdn-HCl. The maximum in the relaxation time corresponds closely with the midpoint in the equilibrium titration for apo-mAS-SOD (Fig. 2), as expected for a simple two-state folding reaction.[38] Extrapolation of both relaxation times, τ, to the absence of denaturant yields rate constants, k ($k=1/\tau$), of $k_u=3.1\times10^{-5}$ s^{-1} for unfolding and $k_f=0.016$ s^{-1} for refolding. The denaturant dependence values of the rate constants, the $m^{\ddagger}$ values, are −1.4 and 3.5 kcal (mol monomer)$^{-1}$ M^{-1}, respectively. The free energy of folding of apo-mAS-SOD, estimated from $\Delta G^0=-RT\ \ln(k_u/k_f)$, is −3.6±0.1 kcal (mol monomer)$^{-1}$, in reasonable agreement with the stability estimated from the equilibrium titration, −4.3±0.1 kcal (mol monomer)$^{-1}$ (Table 1).

The kinetic consequences of unfolding and refolding mAS-SOD in the presence of stoichiometric zinc are to increase the unfolding relaxation time by ~110-fold at 3 M Gdn-HCl and to decrease the refolding relaxation time by ~100-fold at 0.6 M Gdn-HCl (Fig. 4B). As in the case of the dimeric AS-SOD, the refolding relaxation time is independent of the zinc concentration at and above stoichiometric zinc concentrations (data not shown). Below stoichiometric zinc concentrations, a small faster phase with a relaxation time equal to that for apo-mAS-SOD appears (data not shown). The two phases reflect the independent folding of the zinc-bound unfolded and zinc-free unfolded AS-SOD. The $m_u^{\ddagger}$ and $m_f^{\ddagger}$ values in the presence of zinc are similar to those in the absence of zinc, ensuring that the differences in the relaxation times observed in Gdn-HCl are maintained in the absence of denaturant.

Preferential binding of zinc to the zinc site in refolding was tested by a double-jump experiment. Metal-free mAS-SOD was unfolded in 3.9 M Gdn-HCl and then refolded by a 10-fold dilution to 0.4 M Gdn-HCl containing stoichiometric zinc. After 30 s of refolding, approximately three times the refolding relaxation time under these conditions (Fig. 4A), the protein was unfolded in 4.2 M Gdn-HCl and the unfolding reaction was monitored by CD. The observed unfolding relaxation time is within error to the observed relaxation time for a single-jump unfolding reaction to the same final conditions when the protein is incubated with stoichiometric zinc in the native state (Fig. 6b). Given the preferential binding of zinc to the zinc site in native AS-SOD (Fig. 4), zinc must also bind preferentially to the zinc site during the refolding reaction.

The obvious perturbations of the unfolding and refolding relaxation times for mAS-SOD at stoichiometric concentrations of monomer and zinc (Fig. 6b) and the knowledge that zinc binds to both folded and unfolded proteins in low concentrations of

denaturant allow a simple two-state analysis of the U▪Zn ⇆ M▪Zn reaction from the chevron. The free energy difference between these states, $\Delta G = -RT \ln (k_u/k_f)$, is -9.0 ± 0.1 kcal (mol monomer)$^{-1}$ in the absence of denaturant. When this value is added to the free energy of binding of zinc to the peptide model of the unfolded state, -8.0 ± 0.3 kcal (mol monomer)$^{-1}$, the free energy of the zinc-bound folded monomeric form relative to the zinc-free unfolded state is found to be -17.0 ± 0.7 kcal (mol monomer)$^{-1}$.

The kinetic chevrons for apo-mAS-SOD and Zn-mAS-SOD also provide a resolution to the anomalously low m value for the equilibrium titration of Zn-mAS-SOD. For two-state reactions, the sum of the absolute values of the kinetic $m^{\ddagger}$ values is equal to the m value for the equilibrium titration. The equilibrium m value for apo-mAS-SOD, 5.1 ± 0.5 kcal (mol monomer)$^{-1}$ M^{-1}, is in good agreement with the value determined from the rate constants for folding and unfolding, 4.9 ± 0.3 kcal (mol monomer)$^{-1}$ M^{-1}. By contrast, the equilibrium m value for Zn-mAS-SOD, 2.6 ± 0.2 kcal (mol monomer)$^{-1}$ M^{-1}, is about half that determined from the chevron for this system, 4.6 ± 0.3 kcal (mol monomer)$^{-1}$ M^{-1}. These contradictory estimates for the equilibrium m value reflect the complexity of the equilibrium Zn-mAS-SOD folding reaction. At equilibrium in the transition zone, the m value is sensitive to the presence of all the states that bind zinc and are significantly populated under these conditions. The kinetic experiment, by contrast, reveals the rate constants for specific steps in the mechanism, U▪Zn → M▪Zn and M▪Zn → U▪Zn, that pass through a common transition-state ensemble (TSE). The sum of the absolute values of the denaturant dependences of these rate constants provides an accurate measure of the equilibrium m value and, with the extrapolated intercepts of the rate constants, an accurate estimate of the stability of Zn-mAS-SOD not available from the equilibrium titration experiment.

The good agreement between the m values for apo-mAS-SOD and Zn-mAS-SOD obtained from the kinetic analysis (Table 2) implies that the buried surface induced by zinc binding is similar for the M·Zn, the U·Zn, and the intervening TSE compared with their respective apo states. If zinc were binding to non-zinc sites in unfolded AS-SOD so as to reduce the equilibrium m value by a factor of 2, one might expect to observe a significant decrease in the $m_f^{\ddagger}$ value for the folding reaction. The very similar $m_f^{\ddagger}$ values for apo- and Zn-mAS-SOD (Fig. 6; Table 2) argue against this possibility.

Reaction coordinate diagram for Zn-AS-SOD

The folding data for the apo- and zinc-bound forms of AS-SOD and mAS-SOD and the thermodynamic data for the binding of zinc to the peptide model of the zinc-binding loop can be combined to determine the effect of zinc on the folding reaction coordinate diagram of AS-SOD under standard-state conditions. The free energies are those for the dimeric systems: $2U \leftrightarrows 2M \leftrightarrows N_2$ for apo-AS-SOD and $2(U\text{▪}Zn) \leftrightarrows 2(M\text{▪}Zn) \leftrightarrows (N\text{▪}Zn)_2$ for Zn-AS-SOD. Although the conversion of the kinetic data to transition-state energies depends on the formalism adopted,[40] the perturbations in the free energies of the transition states induced by zinc binding should, to a first approximation, be independent of the formalism because the same kinetic mechanisms are operative.

The procedure by which the thermodynamic and kinetic data on the folding of Zn-AS-SOD were converted into a reaction coordinate diagram was as follows:

1. The unfolded apo-monomer, 2U, was chosen as the reference state for both the apo-AS-SOD and Zn-AS-SOD diagrams (Fig. 7).

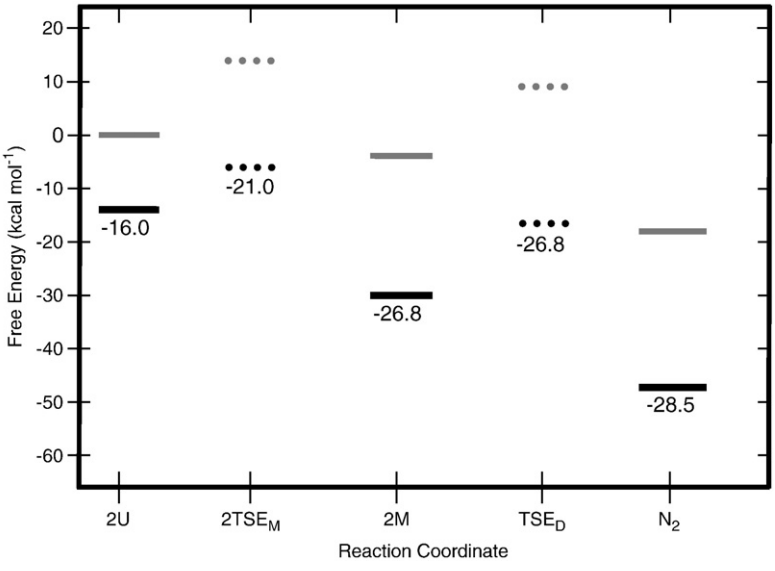

Fig. 7. Reaction coordinate diagrams of apo-AS-SOD and Zn-AS-SOD in the dimer reference frame and at the standard state, 1 M in each of the components. Apo states are depicted in gray, while zinc-bound states are shown in black. Continuous lines are thermodynamic states, where 2U is the unfolded state, 2M is the folded monomer, and N_2 is the native dimer. Dotted lines represent the energies of the transition states, where $2TSE_M$ is the TSE of monomer folding and TSE_D is the TSE of dimer formation. The absolute values of the TSE energies depend on the formalism chosen to determine these energies. All changes in free energy induced by zinc binding, reported under the bar representing the zinc-bound states, are given in kcal (mol dimer)$^{-1}$ units.

2. The energy of the unfolded zinc-bound monomer, U▪Zn, relative to the U state was determined by converting the dissociation constant for the zinc–peptide complex using $\Delta G = -RT \ln(K_d) = -8.0$ kcal (mol monomer)$^{-1}$ (Table 1). For the dimeric system, the free energy of the 2(U·Zn) state is −16.0 kcal (mol dimer)$^{-1}$ lower than that of the 2U state.
3. The chevron analysis of apo-mAS-SOD (Fig. 6b) revealed that the folded monomeric state, 2M, is −7.2 kcal (mol dimer)$^{-1}$ lower than the 2U state.[28] The thermodynamic stability of Zn-mAS-SOD was calculated by fitting its kinetic chevron to a two-state model, and the free energy difference between the U▪Zn ⇆ N▪Zn states was determined from $\Delta G^0 = -RT \ln(k_u/k_f)$ to be −9.0 kcal (mol monomer)$^{-1}$. The binding free energy of zinc to the unfolded state, U + Zn ⇆ U▪Zn, 8.0 kcal (mol monomer)$^{-1}$, was added to yield a total free energy for the U + Zn ⇆ U▪Zn ⇆ N▪Zn reaction of −17.0 kcal (mol monomer)$^{-1}$. The energy of the 2(M▪Zn) state is −34.0 kcal (mol dimer)$^{-1}$ lower than the 2U state and is −26.8 kcal (mol dimer)$^{-1}$ less than that of the 2M state. Therefore, Zn-mAS-SOD is 13.4 kcal (mol monomer)$^{-1}$ more stable than apo-mAS-SOD (Table 1).
4. The free energy of the $(N▪Zn)_2$ state was calculated by the sum of twice the free energy of Zn-mAS-SOD and the free energy change for the dimerization reaction. The latter free energy change was calculated from the dissociation rate constant, $k_d = 2.1 \times 10^{-5}$ s^{-1}, obtained by linear extrapolation of the unfolding relaxation time at high denaturant concentration (Fig. 6a) and the association rate constant, $k_a = 6.9 \times 10^6$ M^{-1} s^{-1}, determined by global kinetic analysis of the urea-denaturation reaction (A.-K. E. Svensson *et al.*, manuscript in preparation). These rate constants yield a $\Delta G^0_{2U/N2} = 2(\Delta G^0_{U/M}) - RT \ln(k_a/k_d) = -49.4$ kcal (mol dimer)$^{-1}$ for the $(N▪Zn)_2$ state relative to the 2U + 2Zn state. The same calculation performed for the metal-free AS-SOD yields a free energy difference of −20.9 kcal (mol dimer)$^{-1}$ for the N_2 state relative to the 2U state. Therefore, the free energy of the $(N▪Zn)_2$ state is 28.5 kcal (mol dimer)$^{-1}$ less than the N_2 state.
5. The activation free energy of the TSE for the 2M ⇆ N_2 reaction, TSE_D, was placed relative to the M state using the Eyring formalism, $\Delta G^‡ = -RT \ln[(k_a h)/k_B T)]$, where k_a is the association rate constant in the absence of denaturant, 6.9×10^6 M^{-1} s^{-1}, h is the Planck constant, k_B is the Boltzmann constant, and T is the absolute temperature; $\Delta G^‡ = 18.2$ kcal (mol dimer)$^{-1}$. The TSE_D for the 2(M▪Zn) ⇆ $(N▪Zn)_2$ reaction, relative to the (M▪Zn) state, is identical with that for the metal-free M state because the association reaction is near-diffusion limited and will therefore not be affected by zinc binding.
6. The activation free energy for the TSE for the 2U ⇆ 2M reaction, $2TSE_M$, can be placed with the rate constant for folding in the absence of denaturant, 0.012 s^{-1}, and the Eyring formalism as described above. Similarly, the $2TSE_M$ for the 2(U▪Zn) ⇆ 2(M▪Zn) reaction can be placed relative to the 2(U▪Zn) state, recognizing that the 100-fold acceleration in folding due to zinc binding corresponds to a decrease in the barrier of 5.0 kcal (mol dimer)$^{-1}$ (Table 2).

It is evident that zinc binding perturbs the entire folding reaction coordinate for AS-SOD. The implications of this observation for the unfolding/aggregation hypothesis for ALS are discussed subsequently.

Discussion

Modulation of the folding free energy surface

The thermodynamic and kinetic data for the effects of zinc binding on the folding and stability of AS-SOD (Tables 1 and 2) provide quantitative answers to the following questions about the role of zinc in protecting cells against the aggregation of partially folded states of SOD:

1. At what stage of the folding reaction does zinc become bound to SOD and potentially offer protection against aggregation? Zinc binds rapidly to the zinc site in the unfolded state with micromolar affinity *in vitro* and remains bound throughout the reaction. The binding of zinc to the peptide model for unfolded SOD provides a ready explanation for its dramatic acceleration of the monomer folding reaction *in vitro* and offers insights into the source of the very slow folding reaction for apo-AS-SOD (see below). The nanomolar concentration of free zinc in cells,[41] however, is not sufficient to saturate the zinc-binding loop segment, and the lifetime of unfolded SOD would be that of the metal-free protein following synthesis on the ribosome.
2. What are the quantitative ramifications of zinc binding on the propensity of the native dimer and the folded monomer to populate, at equilibrium, less well-structured states that may be prone to aggregate? Zinc binding significantly stabilizes the native dimer and folded monomer relative to the unfolded state by comparable amounts, −28.5±1.8 and −26.8±0.8 kcal (mol dimer)$^{-1}$, respectively, at the standard state of 1 M in each component. The calculated zinc dissociation constants (Table 1) are within the range of 10^{-8} to 10^{-14} M^{-1}, which have been reported previously.[11,12] The wide range of affinities is likely the result of different buf-

fer conditions used. Correcting to a 10 μM standard state, subtracting $-RT$ ln[protein] = +6.7 kcal (mol monomer)$^{-1}$ for mAS-SOD and $-3RT$ ln[protein] = +20.1 kcal (mol dimer)$^{-1}$ for AS-SOD, the zinc-bound monomer is stabilized 6.7 kcal (mol monomer)$^{-1}$ relative to the metal-free monomer state and the relative population of the metal-free monomer would decrease by 10^5-fold. Zinc stabilizes dimeric AS-SOD by 14.8 kcal (mol dimer)$^{-1}$, corresponding to a decrease in the relative population of the metal-free dimer of 10^{11}. Thus, the effects of zinc binding on all the species in the reaction coordinate diagram are dramatic. Mulligan *et al.*[42] have recently demonstrated that the major unfolding pathway of SOD at high concentrations of Gdn-HCl involves the initial dissociation of the dimer coupled with zinc release. Subsequently, the monomer unfolds and copper is released.[42] The results of this study may appear surprising given the very high affinity of SOD for zinc at neutral pH. However, as acknowledged by the authors, zinc dissociation could occur either during dimer dissociation or subsequently via a rapid reaction. The results of the present study support the latter possibility in that zinc dissociation from the unfolded state, U, follows the rate-limiting dimer dissociation reaction and the faster monomer unfolding reaction.

3. Does zinc binding alter the relative populations of monomeric and dimeric forms of SOD at equilibrium? Although the propagation of error analysis finds the stabilities of monomeric and dimeric AS-SOD to be comparable (Table 1), the 20-fold slower dissociation of Zn-AS-SOD *versus* AS-SOD shows that zinc actually stabilizes dimeric AS-SOD, relative to mAS-SOD, by 1.7 kcal (mol dimer)$^{-1}$. The lower free energy for the $(N{\cdot}Zn)_2$ state relative to the 2(M·Zn) state means that the equilibrium between the monomeric and dimeric zinc-bound states will shift to favor the native dimer of AS-SOD in the presence of zinc. Although the major protective effect of zinc binding on SOD would be to decrease the relative populations of metal-free forms, the decrease in the population of the zinc-bound folded monomeric form might also be a factor.

Implications for aggregation

The capacity of all the components in the folding mechanism of wild-type SOD, including the TSEs, to bind zinc has significant implications for the aggregation propensity of ALS-inducing variants. It has been shown that zinc-bound SOD is very resistant to aggregation, reinforcing the structural and protective role of zinc.[43] Two distinct scenarios for aggregation can be envisioned, an equilibrium scenario and a kinetic scenario. The equilibrium scenario involves fully folded disulfide-bonded protein occasionally sampling partially folded or unfolded aggregation-prone states, whereas the kinetic scenario involves the aggregation of transient folding intermediates that are highly populated during the folding reaction following synthesis on the ribosome.

Equilibrium scenario

The subnanomolar binding of zinc to native dimeric SOD, coupled with the intrinsic affinity of the metal-free subunits for each other,[28] means that the coupled equilibria will flow toward the dimeric state for the wild-type protein. As a result, the populations of all zinc-free states will decrease. Conversely, ALS variants containing mutations that lead to the loss of metal binding[44] will shift their populations toward zinc-free monomeric states. For example, the population of the monomeric metal-free form of AS-SOD would increase by 20-fold relative to its metal-bound wild-type counterpart for a 10 μM concentration of the metal-binding variants. Due to the higher-order nature of aggregation reactions, even small changes in the concentration of these aggregation-prone species can be amplified into a large change in the rate of aggregation.

One possible scenario is partial unfolding of the monomeric intermediate state, leaving the protein susceptible to aggregation. Richardson and Richardson[45] as well as Nordlund and Oliveberg[46] have argued that β5 and β6, edge strands in the β-sandwich (Fig. 1), serve as gatekeepers for the β-sandwich by preventing the aggregation of the monomeric species. The boundary position of these two β-strands would make them logical candidates for spontaneous dissociation in a rapidly interconverting ensemble of conformers in a manifold of states representing the folded monomer of SOD. Supporting this model are molecular dynamics simulations that have predicted that mutations and dimer destabilization have the effect of partially unfolding β5 and β6.[47] The disorder induced in the zinc-binding and electrostatic loops in the absence of zinc could propagate to the adjacent β5 strand (Fig. 1) and thereby enhance the propensity for aggregation of monomeric SOD in the absence of zinc. The increased tendency for metal-free ALS variants to bind hydrophobic dyes may be a manifestation of this phenomenon.[48]

Alternatively, the unfolded state could provide a platform for aggregation. The micromolar affinity of the unfolded state for zinc and the subnanomolar affinities (Table 1) of the folded monomeric and dimeric states of AS-SOD mean that the unfolded state will not bind zinc, but the folded monomeric intermediate and the dimeric native state will be saturated at nanomolar concentrations of zinc *in vivo*[41] for the wild-type protein. The folded states of metal-binding variants, which would not be stabilized by metal binding, will not benefit from this shift in equilibrium for the wild-type protein toward

more folded states in the presence of zinc. Once again, this effect will be amplified in the rate of aggregation by the higher-order kinetics that characterize multicomponent reactions.

Kinetic scenario

Arguments have also been made for a kinetic pathway for aggregation, where polypeptide chains misfold and aggregate after synthesis.[49] The micromolar dissociation constant for zinc binding to a peptide model for unfolded SOD means that the folding reaction cannot be accelerated and the lifetime of the unfolded state decreased by nanomolar zinc concentrations *in vivo*. The increased temperature in motor neurons, 37 *versus* 20 °C *in vitro*, would only serve to decrease the affinity of zinc for the unfolded state because zinc binding is exothermic.[11] As a result, immediately following synthesis on the ribosome, zinc would not be expected to offer protection against aggregation of unfolded disulfide-reduced ALS-inducing variants of SOD.

Implications for the folding mechanism of SOD

The significant acceleration of the monomer folding rate by the binding of zinc to unfolded AS-SOD provides insights into the structure of the TSE_M. A previous mutational analysis of monomeric SOD revealed that β1–β4 and β7, representing contributions from both sides of the β-sandwich (β1/β2/β3 and β4/β7; Fig. 1), are integral components of the TSE_M.[45] A surprising property of the zinc-free monomer folding reaction is its very small rate constant, 0.012 s^{-1} (Table 2). This value is $\sim 10^4$ less than the rate constant predicted by the relative contact order, a measure of the sequence separation between contacting residues in the native structure, of the fully folded SOD monomer.[50] This significant discrepancy shows an important aspect of the rate-limiting folding reaction is not captured by this topological metric. The 100-fold acceleration of this reaction by zinc suggests that disorder in the zinc-binding loop might be partially responsible. Application of an algorithm to assess the propensity for disorder, PONDR,[51] to the SOD sequence reveals that the zinc-binding loop and, to a lesser extent, the electrostatic loop as well as β5 and β6 are expected to be natively disordered. The prediction for disorder in the loops and in β5 is in accord with experimental observations on monomeric SOD.[8,9] Both of these loops follow β-strands that are adjacent and integral to the β-sheet on one side of the β-sandwich, β4 and β7, and these loops pack on each other in the fully folded structure (Fig. 1). Thus, the preorganization of the zinc-binding loop in the presence of zinc and its potential recruitment of the electrostatic loop might be expected to enhance the probability of accessing the crucial β4/β7 pair of strands in the TSE_M. The significance of C-terminal organization is also consistent with slower refolding kinetics observed for disulfide-reduced SOD,[26] in which the cross-link between C57 and C146 near the C-terminus is absent. It would be interesting to test the proposed involvement of the zinc and electrostatic loops in the TSE_M by performing a mutational analysis on side chains in these loops in the presence and in the absence of zinc.

Overview on ALS-inducing variants of SOD

The biophysical analyses presented previously[29,45,52,53] support a general mechanism for the gain of function via aggregation of partially folded states whose populations are enhanced in ALS-inducing variants of SOD. As would be expected for a highly cooperative system, the contributions of the inherent protein stability, the disulfide bond, and the affinity for metal binding are strongly coupled.[27,54] This coupling is evident in the present study by the enhanced binding of zinc along the reaction coordinate. It is also evident in previous studies by the loss of affinity for zinc of aggregation-prone ALS variants[44] and by the increased susceptibility of ALS variants for disulfide-bond reduction.[55] Although chaperones and proteosomes may mitigate the potential for aggregation, the diminished potency of these housekeeping systems in aging cells[56–58] may eventually lead to the formation of toxic aggregates by either the thermodynamic scenario or the kinetic scenario. Detailed analyses on the stability and folding of ALS-inducing variants of SOD would provide quantitative metrics on the properties of the unfolded and monomeric intermediate states for comparisons with biological measures of aggregation and toxicity. These experiments are currently in progress.

Materials and Methods

Protein purification

Human AS-SOD and the monomeric variant C6A/C111S/G50E/F51E SOD recombinant proteins were expressed in pET3d/BL21-Gold(DE3) *Escherichia coli* cells (Stratagene®, Inc., Cedar Creek, TX) induced with 1 mM IPTG. All centrifugation steps were done using a Beckman JA 25.50 rotor and performed for 45 min at 4 °C unless otherwise specified. The cells were pelleted by centrifugation at 9000 rpm for 15 min and resuspended in lysis buffer [100 mM Hepes, pH 7.2, 150 mM NaCl, 1 mM $ZnSO_4$, 1 mM dithioerythritol, 1 mg mL^{-1} of lysozyme, and one protease inhibitor tablet (F. Hoffmann, La Roche, Ltd., Switzerland)] per 50 mL of lysate. After being stirred for 30 min at room temperature, the cells were sonicated (30 s on, 90 s off) and centrifuged at 20,000 rpm. The resulting pellet was then resuspended in lysis buffer lacking lysozyme, 0.6 mL per gram of pellet, and the sonication and centrifugation steps were repeated. The combined supernatants were placed in a 47 °C water bath, incubated for 45 min, and then centrifuged at 20,000 rpm (this step was not performed for mAS-SOD). The supernatant from the heat incubation was allowed to cool to room temperature, mixed with an equal volume of 4 M $(NH_4)_2SO_4$, stirred at room temperature for 30 min, and centrifuged at 20,000 rpm.

The resulting supernatant was dialyzed extensively against standard buffer (20 mM Hepes, pH 7.2), loaded onto a Q-Sepharose column, and eluted with a linear gradient to 40% high salt buffer (300 mM KCl and 20 mM Hepes, pH 7.2) over 10 column volumes. The presence of AS-SOD in the fractions was determined by SDS-PAGE. The pooled fractions were concentrated to <10 mL using a YM-10 membrane on an Amicon® concentrator and dialyzed against standard buffer. The protein was demetallated and tested for purity as previously described.[28] The concentration of protein was calculated using a molar extinction coefficient at 280 nm of 5400 M^{-1} cm^{-1} for the monomer of AS-SOD, and, unless otherwise specified, all protein concentrations are given in terms of moles of monomer of AS-SOD per liter of solution.

Peptide labeling and purification

The peptide fragment representing the metal-binding region of loop IV, amino acids 61–86, was purchased from Sigma-Aldrich and modified by adding an N-terminal tryptophan and a C-terminal cysteine. Purity was assessed by a single high-pressure liquid chromatography peak and by mass spectroscopy provided by the manufacturer. The covalent modification of the cysteine with the FRET acceptor IAEDANS [5-((((2-iodoacetyl)amino)ethyl) amino)naphthalene-1-sulfonic acid] was performed at a peptide concentration of 1 mg mL^{-1} in standard buffer with the addition of 1 mM TCEP [Tris(2-carboxyethyl) phosphine]. Initially, 10-fold excess free IAEDANS was incubated with the peptide at room temperature for 2 h. Another 10-fold excess of label was then added, and the reaction mixture was incubated for another 2 h at 4 °C. The labeled peptide was separated from free dye by running the reaction mixture on a 5-mL HiTrap™ desalting column (GE Healthcare Life Sciences).

Equilibrium folding experiments

All CD spectroscopic measurements were performed on a Jasco-810 spectropolarimeter (Jasco Inc., Easton, MD) equipped with a water-cooled Peltier temperature control system. The Gdn-HCl-induced unfolding curves were monitored from 220 to 240 nm in a 0.5-cm path-length quartz cuvette using a scan rate of 20 nm min^{-1} and a response time of 8 s. The change in ellipticity as a function of zinc concentration was monitored using a stepwise scan at a rate of 1 nm per 8 s to enhance signal to noise. Gdn-HCl concentrations were determined by refractive index[59] on a Leica Mark II refractometer. Unless otherwise stated, titration samples were made from concentration-matched stocks of folded protein in buffer and unfolded protein at 7 M Gdn-HCl and incubated at room temperature for 1 day for apo-AS-SOD and for 7 days for zinc-bound protein. Coincident unfolding and refolding curves from companion experiments in which denaturant was added to native protein and buffer was added to unfolded protein ensured that the samples were fully equilibrated in this timeframe. The stocks were mixed precisely using a Hamilton Microlab 500 titrator interfaced with in-house software to calculate the mixing ratios, and the index of refraction of each sample was measured after the experiment was completed. The protein concentrations, given in monomer units, were 10 μM for AS-SOD and 5 μM for mAS-SOD for the equilibrium unfolding experiments.

Kinetic experiments

The unfolding and refolding kinetics of AS-SOD, initiated by manual mixing, were monitored by CD. Data were collected at 230 nm in a 1-cm^2 cuvette under continuous mixing with a solution volume of 1.8–2.0 mL. Unfolding jumps were initiated from protein in 0 M Gdn-HCl, and refolding jumps were initiated from protein denatured overnight in 5–6 M Gdn-HCl to various final concentrations. For zinc-loaded samples, the protein was incubated in stoichiometric zinc prior to dilution in the buffer. The final concentration of Gdn-HCl was measured by index of refraction. Protein concentrations were 10 μM for both AS-SOD and mAS-SOD for the kinetic folding experiments.

Analysis of equilibrium folding data

To determine the folding free energy of metal-free AS-SOD and mAS-SOD from the equilibrium unfolding titrations, we fit the data to a simple two-state mechanism. While it is known that SOD folds via a monomeric intermediate,[26,28,30] it is not populated significantly at these protein concentrations,[29] making a two-state folding model an adequate approximation. For all thermodynamic analyses, the free energy of folding in the absence of denaturant was calculated assuming a linear dependence of the apparent free energy on the denaturant concentration. Equilibrium data were analyzed by globally fitting the CD signal at 20 wavelengths (220–240 nm) to the same thermodynamic parameters. All data were fit using Savuka 6.2, an in-house nonlinear least-squares program using the Levenberg–Marquardt algorithm.[60] In the absence of zinc, equilibrium folding data were fit to a two-state model, $U \leftrightarrows N$ for mAS-SOD and $2U \leftrightarrows N_2$ for AS-SOD as previously described.[28]

For equilibrium titrations in the presence of zinc, the data were modeled as a three-state reaction.

$$U + Zn \rightleftarrows U{\cdot}ZnN{\cdot}Zn$$
$$2U + 2Zn \rightleftarrows 2(U{\cdot}Zn)(N{\cdot}Zn)_2$$

The Gdn-HCl-induced unfolding transition for these titrations involves the native zinc-bound monomer (N▪Zn), or dimer $(N{\blacksquare}Zn)_2$, state, the zinc-bound unfolded U▪Zn, or 2 (U▪Zn), state, and the zinc-free unfolded chains U + Zn and 2U + 2Zn. The equilibrium constants can be defined for the stable monomeric form, Zn-mAS-SOD, as:

$$K_d = \frac{[U][Zn]}{[U{\cdot}Zn]},\ K_u = \frac{[U{\cdot}Zn]}{[N{\cdot}Zn]}$$

and for the dimeric form, Zn-AS-SOD, as:

$$K_d = \frac{[U]^2[Zn]^2}{[U{\cdot}Zn]^2},\ K_u = \frac{[U{\cdot}Zn]^2}{[N{\cdot}Zn]}$$

An equation for total protein concentration may be written as a function of K_u, the equilibrium constant of unfolding, K_d, the dissociation constant for zinc, the total protein concentration (P_t), the total zinc concentration (Z_t), and the concentration of unfolded protein ([U]) (see Supplementary Data for a more detailed derivation).

Zn-mAS-SOD:

$$P_t = \frac{[U]{\cdot}Z_t}{[U] + [U]{\cdot}K_u + K_u{\cdot}K_d} + \frac{[U]{\cdot}Z_t}{[U] + K_d + \frac{[U]}{K_u}} + [U]$$

Zn-AS-SOD:

$$P_t = \frac{2 \cdot [U]^2 \cdot x^2}{K_u \cdot K_d^2} + \frac{[U]}{K_d} \cdot x + [U], \text{ where}$$

$$x = \frac{-[U]}{K_d} - 1 + \sqrt{\frac{\left(\frac{[U]}{K_d} + 1\right)^2 + \frac{8 \cdot [U]^2 \cdot Z_t}{K_u \cdot K_d^2}}{\frac{4 \cdot [U]^2}{K_u \cdot K_d^2}}}$$

The titration data were fit by numerically solving the equations for the concentration of unfolded protein at each Gdn-HCl concentration. The values for K_d and its denaturant dependence were held fixed to the values obtained from an independent assessment of the zinc–peptide complex, and the value for K_u was optimized across the denaturant concentration and the wavelength range, 220–240 nm. The free energy differences between thermodynamic states were assumed to depend linearly on the Gdn-HCl concentration.

Analysis of kinetic folding data

The unfolding and refolding relaxation times were obtained by jumping from 0 or 6 M Gdn-HCl to various final concentrations of denaturant and fitting the traces to exponentials as described previously.[28] The monomer folding and unfolding rates, for both apo- and Zn-mAS-SOD in the absence of denaturant, were calculated by fitting the chevron to a two-state folding model:

$$k = k_f e^{(-m_f[D]/RT)} + k_u e^{(-m_u[D]/RT)}$$

Where k is the observed rate constant; k_f and k_u are the folding and unfolding rate constants in the absence of denaturant, respectively; m_f and m_u are the denaturant dependence of the folding and unfolding rates, respectively; [D] is the denaturant concentration; R is the gas constant; and T is the absolute temperature. Knowing the folding and unfolding rate constants in the absence of denaturant, the folding free energy can be calculated as:

$$\Delta G_u = -RT\ln\left(\frac{k_u}{k_f}\right)$$

The dimer dissociation rate constants in the absence of denaturant were calculated from linear extrapolations to 0 M Gdn-HCl of the >5.5 M Gdn-HCl region of the unfolding leg of the Zn-AS-SOD chevron and the >3.8 M Gdn-HCl region of the unfolding leg of the apo-AS-SOD chevron.

Analysis of zinc binding to the zinc-binding loop peptide

All fluorescence spectroscopic measurements were done on a T-format Spex Fluorolog-3 (Instruments SA, Inc., Edison, NJ) at room temperature. The donor tryptophan was excited at 280 nm, and the emission spectra were monitored from 320 to 540 nm to encompass both the tryptophan and AEDANS fluorescence. The peptide was incubated at various concentrations of Gdn-HCl ranging from 0 to 6 M in standard buffer. Zinc was added in a stepwise manner, from a high-concentration stock solution to minimize changes to the volume to samples at each denaturant concentration. The fluorescence spectra were obtained at various zinc and denaturant concentrations and corrected for background fluorescence and the small change in volume accompanying the addition of zinc. The fluorescence was measured as a function of zinc concentration, and all wavelengths were simultaneously fit to a binding isotherm with one binding site per peptide:

$$y = \frac{B_{max} \times [Zn]}{K_d + [Zn]}$$

where y is the fluorescence intensity, B_{max} is the signal at saturating concentrations of zinc, K_d is the dissociation equilibrium constant; and [Zn] is the concentration of zinc.

Acknowledgements

This work was supported by the National Institutes of Health through grant GM 54836 (awarded to C.R.M). We thank Drs. Osman Bilsel, Anna-Karin E. Svensson, Lawrence Hayward, and Ashutosh Tiwari for their stimulating discussions and input during this project. We also thank Dr. James Evans and the personnel at the Proteomics and Mass Spectrometry Core Facility of Massachusetts Medical School for the molecular weight and protein purity determinations.

Supplementary Data

Supplementary data associated with this article can be found, in the online version, at doi:10.1016/j.jmb.2008.09.045

References

1. Rowland, L. P. & Shneider, N. A. (2001). Amyotrophic lateral sclerosis. *N. Engl. J. Med.* **344**, 1688–1700.
2. Rosen, D. R., Siddique, T., Patterson, D., Figlewicz, D. A., Sapp, P., Hentati, A. *et al.* (1993). Mutations in Cu/Zn superoxide dismutase gene are associated with familial amyotrophic lateral sclerosis. *Nature*, **362**, 59–62.
3. Andersen, P. M., Sims, K. B., Xin, W. W., Kiely, R., O'Neill, G., Ravits, J. *et al.* (2003). Sixteen novel mutations in the Cu/Zn superoxide dismutase gene in amyotrophic lateral sclerosis: a decade of discoveries, defects and disputes. *Amyotrophic Lateral Scler. Other Motor Neuron Disord.* **4**, 62–73.
4. McCord, J. M. & Fridovich, I. (1969). Superoxide dismutase. An enzymic function for erythrocuprein (hemocuprein). *J. Biol. Chem.* **244**, 6049–6055.
5. Strange, R. W., Antonyuk, S. V., Hough, M. A., Doucette, P. A., Valentine, J. S. & Hasnain, S. S. (2006). Variable metallation of human superoxide dismutase: atomic resolution crystal structures of Cu–Zn, Zn–Zn and as-isolated wild-type enzymes. *J. Mol. Biol.* **356**, 1152–1162.
6. Parge, H. E., Hallewell, R. A. & Tainer, J. A. (1992). Atomic structures of wild-type and thermostable mutant recombinant human Cu,Zn superoxide dismutase. *Proc. Natl Acad. Sci. USA*, **89**, 6109–6113.
7. Roberts, B. R., Tainer, J. A., Getzoff, E. D., Malencik, D. A., Anderson, S. R., Bomben, V. C. *et al.* (2007).

Structural characterization of zinc-deficient human superoxide dismutase and implications for ALS. *J. Mol. Biol.* **373**, 877–890.
8. Banci, L., Bertini, I., Cramaro, F., DelConte, R. & Viezzoli, M. S. (2003). Solution structure of apo Cu,Zn superoxide dismutase: role of metal ions in protein folding. *Biochemistry*, **42**, 9543–9553.
9. Strange, R. W., Antonyuk, S., Hough, M. A., Doucette, P. A., Rodriguez, J. A., Hart, P. J. *et al.* (2003). The structure of holo and metal-deficient wild-type human Cu,Zn superoxide dismutase and its relevance to familial amyotrophic lateral sclerosis. *J. Mol. Biol.* **328**, 877–891.
10. Banci, L., Bertini, I., Cantini, F., D'Onofrio, M. & Viezzoli, M. S. (2002). Structure and dynamics of copper-free SOD: the protein before binding copper. *Protein Sci.* **11**, 2479–2492.
11. Potter, S. Z., Zhu, H., Shaw, B. F., Rodriguez, J. A., Doucette, P. A., Sohn, S. H. *et al.* (2007). Binding of a single zinc ion to one subunit of copper–zinc superoxide dismutase apoprotein substantially influences the structure and stability of the entire homodimeric protein. *J. Am. Chem. Soc.* **129**, 4575–4583.
12. Crow, J. P., Sampson, J. B., Zhuang, Y., Thompson, J. A. & Beckman, J. S. (1997). Decreased zinc affinity of amyotrophic lateral sclerosis-associated superoxide dismutase mutants leads to enhanced catalysis of tyrosine nitration by peroxynitrite. *J. Neurochem.* **69**, 1936–1944.
13. Furukawa, Y. & O'Halloran, T. V. (2006). Posttranslational modifications in Cu,Zn-superoxide dismutase and mutations associated with amyotrophic lateral sclerosis. *Antioxid. Redox Signal.* **8**, 847–867.
14. Valentine, J. S. & Hart, P. J. (2003). Misfolded CuZnSOD and amyotrophic lateral sclerosis. *Proc. Natl Acad. Sci. USA*, **100**, 3617–3622.
15. Cleveland, D. W. & Rothstein, J. D. (2001). From Charcot to Lou Gehrig: deciphering selective motor neuron death in ALS. *Nat. Rev. Neurosci.* **2**, 806–819.
16. Wood, J. D., Beaujeux, T. P. & Shaw, P. J. (2003). Protein aggregation in motor neurone disorders. *Neuropathol. Appl. Neurobiol.* **29**, 529–545.
17. Bruijn, L. I., Miller, T. M. & Cleveland, D. W. (2004). Unraveling the mechanisms involved in motor neuron degeneration in ALS. *Annu. Rev. Neurosci.* **27**, 723–749.
18. Caughey, B. & Lansbury, P. T. (2003). Protofibrils, pores, fibrils, and neurodegeneration: separating the responsible protein aggregates from the innocent bystanders. *Annu. Rev. Neurosci.* **26**, 267–298.
19. Stefani, M. & Dobson, C. M. (2003). Protein aggregation and aggregate toxicity: new insights into protein folding, misfolding diseases and biological evolution. *J. Mol. Med.* **81**, 678–699.
20. Valentine, J. S., Doucette, P. A. & Zittin Potter, S. (2005). Copper–zinc superoxide dismutase and amyotrophic lateral sclerosis. *Annu. Rev. Biochem.* **74**, 563–593.
21. Ross, C. A. & Poirier, M. A. (2004). Protein aggregation and neurodegenerative disease. *Nat. Med.* **10**, S10–S17.
22. Khare, S. D., Caplow, M. & Dokholyan, N. V. (2004). The rate and equilibrium constants for a multistep reaction sequence for the aggregation of superoxide dismutase in amyotrophic lateral sclerosis. *Proc. Natl Acad. Sci. USA*, **101**, 15094–15099.
23. Hart, P. J. (2006). Pathogenic superoxide dismutase structure, folding, aggregation and turnover. *Curr. Opin. Chem. Biol.* **10**, 131–138.
24. Cao, X., Antonyuk, S., Seetharaman, S. V., Whitson, L. J., Taylor, A. B., Holloway, S. P. *et al.* (2008). Structures of the G85R variant of SOD1 in familial ALS. *J. Biol. Chem.* **283**, 16169–16177.
25. Lindberg, M. J., Bystrom, R., Boknas, N., Andersen, P. M. & Oliveberg, M. (2005). Systematically perturbed folding patterns of amyotrophic lateral sclerosis (ALS)-associated SOD1 mutants. *Proc. Natl Acad. Sci. USA*, **102**, 9754–9759.
26. Lindberg, M. J., Normark, J., Holmgren, A. & Oliveberg, M. (2004). Folding of human superoxide dismutase: disulfide reduction prevents dimerization and produces marginally stable monomers. *Proc. Natl Acad. Sci. USA*, **101**, 15893–15898.
27. Hornberg, A., Logan, D. T., Marklund, S. L. & Oliveberg, M. (2007). The coupling between disulphide status, metallation and dimer interface strength in Cu/Zn superoxide dismutase. *J. Mol. Biol.* **365**, 333–342.
28. Svensson, A. K., Bilsel, O., Kondrashkina, E., Zitzewitz, J. A. & Matthews, C. R. (2006). Mapping the folding free energy surface for metal-free human Cu, Zn superoxide dismutase. *J. Mol. Biol.* **364**, 1084–1102.
29. Vassall, K. A., Stathopulos, P. B., Rumfeldt, J. A., Lepock, J. R. & Meiering, E. M. (2006). Equilibrium thermodynamic analysis of amyotrophic lateral sclerosis-associated mutant apo Cu,Zn superoxide dismutases. *Biochemistry*, **45**, 7366–7379.
30. Rumfeldt, J. A., Stathopulos, P. B., Chakrabarrty, A., Lepock, J. R. & Meiering, E. M. (2006). Mechanism and thermodynamics of guanidinium chloride-induced denaturation of ALS-associated mutant Cu,Zn superoxide dismutases. *J. Mol. Biol.* **355**, 106–123.
31. Hallewell, R. A., Imlay, K. C., Lee, P., Fong, N. M., Gallegos, C., Getzoff, E. D. *et al.* (1991). Thermostabilization of recombinant human and bovine CuZn superoxide dismutases by replacement of free cysteines. *Biochem. Biophys. Res. Commun.* **181**, 474–480.
32. Lindberg, M. J., Tibell, L. & Oliveberg, M. (2002). Common denominator of Cu/Zn superoxide dismutase mutants associated with amyotrophic lateral sclerosis: decreased stability of the apo state. *Proc. Natl Acad. Sci. USA*, **99**, 16607–16612.
33. Bertini, I., Piccioli, M., Viezzoli, M. S., Chiu, C. Y. & Mullenbach, G. T. (1994). A spectroscopic characterization of a monomeric analog of copper, zinc superoxide dismutase. *Eur. Biophys. J.* **23**, 167–176.
34. Lyons, T. J., Nersissian, A., Huang, H., Yeom, H., Nishida, C. R., Graden, J. A. *et al.* (2000). The metal binding properties of the zinc site of yeast copper–zinc superoxide dismutase: implications for amyotrophic lateral sclerosis. *J. Biol. Inorg. Chem.* **5**, 189–203.
35. Pozdnyakova, I., Guidry, J. & Wittung-Stafshede, P. (2001). Probing copper ligands in denatured *Pseudomonas aeruginosa* azurin: unfolding His117Gly and His46Gly mutants. *J. Biol. Inorg. Chem.* **6**, 182–188.
36. Wittung-Stafshede, P. (2002). Role of cofactors in protein folding. *Acc. Chem. Res.* **35**, 201–208.
37. Myers, J. K., Pace, C. N. & Scholtz, J. M. (1995). Denaturant *m* values and heat capacity changes: relation to changes in accessible surface areas of protein unfolding. *Protein Sci.* **4**, 2138–2148.
38. Matthews, C. R. (1987). Effect of point mutations on the folding of globular proteins. *Methods Enzymol.* **154**, 498–511.
39. Pace, C. N., Shirley, B. A. & Thompson, J. A. (1990). Measuring the conformational stability of a protein. In *Protein Structure : A Practical Approach*, 2nd edit. IRL Press at Oxford University Press, Oxford, UK.
40. Bodenreider, C. & Kiefhaber, T. (2005). Interpretation of protein folding psi values. *J. Mol. Biol.* **351**, 393–401.

41. Choi, D. W. & Koh, J. Y. (1998). Zinc and brain injury. *Annu. Rev. Neurosci.* **21**, 347–375.
42. Mulligan, V. K., Kerman, A., Ho, S. & Chakrabartty, A. (2008). Denaturational stress induces formation of zinc-deficient monomers of Cu,Zn superoxide dismutase: implications for pathogenesis in amyotrophic lateral sclerosis. *J. Mol. Biol.* **383**, 424–436.
43. Banci, L., Bertini, I., Durazo, A., Girotto, S., Gralla, E. B., Martinelli, M. *et al.* (2007). Metal-free superoxide dismutase forms soluble oligomers under physiological conditions: a possible general mechanism for familial ALS. *Proc. Natl Acad. Sci. USA*, **104**, 11263–11267.
44. Hayward, L. J., Rodriguez, J. A., Kim, J. W., Tiwari, A., Goto, J. J., Cabelli, D. E. *et al.* (2002). Decreased metallation and activity in subsets of mutant superoxide dismutases associated with familial amyotrophic lateral sclerosis. *J. Biol. Chem.* **277**, 15923–15931.
45. Richardson, J. S. & Richardson, D. C. (2002). Natural beta-sheet proteins use negative design to avoid edge-to-edge aggregation. *Proc. Natl Acad. Sci. USA*, **99**, 2754–2759.
46. Nordlund, A. & Oliveberg, M. (2006). Folding of Cu/Zn superoxide dismutase suggests structural hotspots for gain of neurotoxic function in ALS: parallels to precursors in amyloid disease. *Proc. Natl Acad. Sci. USA*, **103**, 10218–10223.
47. Khare, S. D. & Dokholyan, N. V. (2006). Common dynamical signatures of familial amyotrophic lateral sclerosis-associated structurally diverse Cu,Zn superoxide dismutase mutants. *Proc. Natl Acad. Sci. USA*, **103**, 3147–3152.
48. Tiwari, A., Xu, Z. & Hayward, L. J. (2005). Aberrantly increased hydrophobicity shared by mutants of Cu, Zn-superoxide dismutase in familial amyotrophic lateral sclerosis. *J. Biol. Chem.* **280**, 29771–29779.
49. Jahn, T. R. & Radford, S. E. (2008). Folding *versus* aggregation: polypeptide conformations on competing pathways. *Arch. Biochem. Biophys.* **469**, 100–117.
50. Plaxco, K. W., Simons, K. T. & Baker, D. (1998). Contact order, transition state placement and the refolding rates of single domain proteins. *J. Mol. Biol.* **277**, 985–994.
51. Romero, P., Obradovic, Z., Li, X., Garner, E. C., Brown, C. J. & Dunker, A. K. (2001). Sequence complexity of disordered protein. *Proteins*, **42**, 38–48.
52. Khare, S. D., Caplow, M. & Dokholyan, N. V. (2006). FALS mutations in Cu,Zn superoxide dismutase destabilize the dimer and increase dimer dissociation propensity: a large-scale thermodynamic analysis. *Amyloid*, **13**, 226–235.
53. Rakhit, R., Crow, J. P., Lepock, J. R., Kondejewski, L. H., Cashman, N. R. & Chakrabartty, A. (2004). Monomeric Cu,Zn-superoxide dismutase is a common misfolding intermediate in the oxidation models of sporadic and familial amyotrophic lateral sclerosis. *J. Biol. Chem.* **279**, 15499–15504.
54. Bruns, C. K. & Kopito, R. R. (2007). Impaired post-translational folding of familial ALS-linked Cu,Zn superoxide dismutase mutants. *EMBO J.* **26**, 855–866.
55. Tiwari, A. & Hayward, L. J. (2003). Familial amyotrophic lateral sclerosis mutants of copper/zinc superoxide dismutase are susceptible to disulfide reduction. *J. Biol. Chem.* **278**, 5984–5992.
56. Zhang, Q., Powers, E. T., Nieva, J., Huff, M. E., Dendle, M. A., Bieschke, J. *et al.* (2004). Metabolite-initiated protein misfolding may trigger Alzheimer's disease. *Proc. Natl Acad. Sci. USA*, **101**, 4752–4757.
57. Massey, A. C., Kiffin, R. & Cuervo, A. M. (2006). Autophagic defects in aging: looking for an "emergency exit"? *Cell Cycle*, **5**, 1292–1296.
58. Derham, B. K. & Harding, J. J. (1997). Effect of aging on the chaperone-like function of human alpha-crystallin assessed by three methods. *Biochem. J.* **328**, 763–768.
59. Thomson, J. A., Shirley, B. A., Grimsley, G. R. & Pace, C. N. (1989). Conformational stability and mechanism of folding of ribonuclease T1. *J. Biol. Chem.* **264**, 11614–11620.
60. Bilsel, O., Zitzewitz, J. A., Bowers, K. E. & Matthews, C. R. (1999). Folding mechanism of the alpha-subunit of tryptophan synthase, an alpha/beta barrel protein: global analysis highlights the interconversion of multiple native, intermediate, and unfolded forms through parallel channels. *Biochemistry*, **38**, 1018–1029.